GSI

GSI - 82 - 27
PREPRINT

Magnetic Moments in the Backbending Region of ^{158}Dy

G. Seiler - Clark, D. Pelte, H. Emling, A. Balanda,
H. Grein, E. Grosse, R. Kulessa, D. Schwalm,
H.J. Wollersheim, M. Hass, G.J. Kumbartzki and K.-H. Speidel

November 1982

Gesellschaft für Schwerionenforschung mbH
Planckstr. 1 · Postfach 110541 · D-6100 Darmstadt 11 · Germany

Magnetic Moments in the Backbending Region of ^{158}Dy

G. Seiler-Clark and D. Pelte
Physikalisches Institut, Univ. Heidelberg, D-6900 Heidelberg, Germany
and
H. Emling, A. Baranda[1], H. Grein, E. Grosse, R. Kulessa[1], D. Schwalm[2]
and H.J. Wollersheim
Gesellschaft für Schwerionenforschung, D-6100 Darmstadt, Germany
and
M. Hass
Weizmann Institute of Science, Rehovot, Israel
and
G.J. Kumbartzki and K.-H. Speidel
Inst. für Strahlen- und Kernphysik, Univ. Bonn,
D-5300 Bonn, Germany

[1] Permanent address: Institute of Physics, Jagiellonian University, 30-059 Krakow, Poland
[2] Present address: Physikalisches Institut, Universität Heidelberg, D-6900 Heidelberg

ABSTRACT

Yrast levels in the backbending region of ^{158}Dy were Coulomb excited with a 4.7 MeV/u ^{208}Pb beam. Employing the transient field technique with a thin magnetized iron foil, the precessions of the angular correlations of decay γ-rays from levels up to spin $I^{\pi} = 16^{+}$ were measured. The results show a clear reduction of the g-factor for states in the backbending region relative to that of the low spin levels, thus demonstrating that the backbending in ^{158}Dy is mainly caused by the alignment of $i_{13/2}$ -neutrons. In a similar experiment, precession measurements on Coulomb excited low spin levels of ^{164}Dy served to determine the static hyperfine field of Dy in Fe and the g-factor of the 6^{+} state in ^{164}Dy.

E [*NUCLEAR REACTIONS* ^{158}Dy(^{208}Pb, ^{208}Pb')^{158}Dy, ^{164}Dy(^{208}Pb, ^{208}Pb')^{164}Dy, E = 4.7 MeV/u; Coulomb excitation; transient field technique; measured W(θ,B); deduced magnetic moments. Enriched targets.]

1. Introduction

Most of the experimental information on the backbending effect, observed in the yrast-sequence of many rare earth nuclei and believed to result from the rotation alignment of a nucleon pair along the axis of collective rotation, stems from the study of energy levels and, to a lesser extent, from E2 transition rates. As for many other rare earth isotopes, in ^{158}Dy the first irregularity in the yrast sequence is observed at spins between $I^{\pi}=14^{+}$ and $I^{\pi}=16^{+}$ (ref. 1); it is understood within the rotation alignment picture (see e.g. ref. 2) as being due to an intersection of the ground state band with a strongly interacting aligned two $i_{13/2}$-neutron quasi-particle band. A recent measurement[3] of B(E2) values between high spin states in ^{158}Dy supports the picture of two crossing, strongly interacting bands with slightly different intrinsic deformations. A measurement of the g-factors of yrast states around backbending, however, would provide a sensitive test of the rotation alignment picture, as this quantitiy is a clear signature of the particles involved and of the amount of spin alignment[4]. In particular, if the backbending is caused by the complete alignment of two $i_{13/2}$ neutrons, a drastic reduction of the g-factors in the backbending region is expected, $g \simeq 0$ as compared to the collective value of $g_c \simeq +0.35$; in contrast, the g-factor is expected to be $g \simeq +1.0$ in case the backbending is caused by the alignment of two $h_{11/2}$ protons.

Most previous attempts to determine magnetic moments of short lived high spin yrast levels in this mass region were hampered by experimental difficulties: In (HI,xn) reactions the complex feeding pattern makes the analysis of the experimental data difficult (see e.g. ref. 5). In Coulomb excitation experiments, on the other hand, the feeding can be controlled, but with projectiles lighter than Pb the high spin states at and above backbending are not accessible because of their weak population. For example, a recent Coulomb excitation experiment with 4.1 MeV/u ^{86}Kr ions[6] could probe the yrast levels of ^{170,174}Yb and ^{160}Dy around spins 8^{+}, 10^{+} and 12^{+} only, with very little sensitivity to the g-factors of the 14^{+} and 16^{+} levels; nevertheless, the precession data indicate a decrease of the magnetic moments with spin, suggestive of an increasing role of aligned neutron configurations in the structure of the yrast states of these nuclei. A really significant deviation from the collective g-factor was obtained recently[7] in a measurement on high spin states in ^{134}Ce. In this case it was demonstrated that $h_{11/2}$ neutrons play the dominant role for the backbending in this nucleus.

The present experiment, undertaken in order to measure g-factors of the yrast states in ^{158}Dy, was designed to be in particular sensitive to the 14^{+} and 16^{+} levels, thus directly probing the backbending region in this nucleus, which has been extensively studied in the UNILAC laboratory

exploiting both the Coulomb excitation process with ^{208}Pb ions[8] and the (HI,xn) reaction using Xe beams[3]. Spectroscopic properties such as lifetimes, population probabilities, etc. are therefore well known and should ensure a straightforward data analysis of the present experiment, free of uncertainties related to the spectroscopy of ^{158}Dy. Low spin levels (up to $I^{\pi}=6^{+}$) in ^{164}Dy were also investigated in the course of this work; these measurements mainly served to calibrate the static hyperfine field of Dy in Fe, which was then used to deduce the g-factors of the low spin states in ^{158}Dy.

2. *Experimental Set-up and Data Reduction*

The experiment is based on measuring the precessions of particle coincident γ-ray angular correlations caused by the transient field that acts on swift ions traversing thin polarized ferromagnetic foils [9]. This technique is especially suited for the purpose of measuring g-factors of levels with lifetimes in the ps range, as is the case for the levels in the region of interest.

The ^{158}Dy yrast levels were populated by Coulomb excitation with 4.7 MeV/u ^{208}Pb projectiles of 1 pnA intensity supplied by the UNILAC accelerator in Darmstadt; a schematic view of the experimental set-up is shown in fig.

1a. The target (fig. 1b) consisted of a layer of 1mg/cm^2 of highly enriched (>98%) ^{158}Dy deposited on a 4.4mg/cm^2 thick iron foil.[+] This was backed by 50µg/cm^2 of Al to prevent the conceivable - though yet unobserved - possibility of polarized electron pick-up of the recoiling Dy ions on emergence from the ferromagnetic foil. The foil was magnetized by an external field of B_{ext} = 0.03 Tesla which was proved to be sufficient for saturation by a magnetometer measurement. The ^{164}Dy measurement was carried out under the same experimental conditions, although only a considerably smaller number of events was collected in this experiment as compared to the ^{158}Dy run.

Recoiling target nuclei and/or scattered particles traversing the iron backing were detected in two position sensitive parallel plate detectors [10] (P_R and P_L in fig. 1a) positioned in the forward hemisphere symmetrically to the beam axis , each subtending an angular range of $20^{\circ} \leq \theta_p \leq 40^{\circ}$ and $\Delta\phi_p = 56^{\circ}$.

The Dy ions were distinguished from recoiling Fe and scattered Pb ions by means of the kinematical correlation between their scattering angles and their flight-times measured relative to the beam burst. Fig. 1c presents a

---

[+] The Dy targets were prepared in the laboratoire R. Bernas (CSNSM), Orsay, France

typical example of such correlations. The Fe, Dy and Pb ions were rather well separated from one another and two-dimensional polygons were used to select the various event types; moreover, the detection of Pb or Dy ions results in considerably different Doppler shifts of the coincident γ-rays. Combining both criteria a complete separation of the different event types could be achieved.

Detected Dy ions correspond to low impact parameter events and hence to the excitation of high spin levels; more precisely they correspond to c.m. scattering angles $\theta_{c.m.}$ of the Pb projectiles of $100^\circ \leq \theta_{c.m.} \leq 140^\circ$. Depending on scattering angles, the initial velocities of the recoiling Dy ions range between 11.5 v_o and 14.1 v_o ($v_o = c/137$) and the corresponding exit velocities between 6.9 v_o and 11.3 v_o. The corresponding transit times t_{tr} through the iron foil of 0.3 to 0.4 ps are short compared to even the shortest lifetimes involved (e.g. $\tau(18^+)$ = .79 ps for ^{158}Dy, ref.3); the precession therefore occurs predominantly in the state directly populated in the Coulomb excitation process. These events shall be referred to as "Dy-events" in the following.

The detection of scattered Pb projectiles is unambiguous with respect to reaction partner as well as impact parameter: The maximum laboratory scattering angle for Pb impinging on iron is less than 16° (and thus outside

the acceptance of the particle detectors), while for the scattering on Dy the Pb energies associated with large c.m. angles are not sufficient for the Pb nuclei to leave the backing foil. By proper choice of the Pb detection angles ($20^\circ \leq \theta_{Pb} \leq 27^\circ$) an impact parameter region is selected where the corresponding Dy ions are stopped in the iron foil. These events correspond to small c.m. angles ($43^\circ \leq \theta_{c.m.} \leq 64^\circ$) and hence to a predominant excitation of lower spin levels. In this case the Dy ions recoil with velocities of $7 \geq v/v_o \geq 0$ in the Fe foil; the stopping times t_s amount to 1.3 ps on the average. These events shall be referred to as "Pb-events".

Gamma rays in coincidence with Dy-events (or Pb-events) were detected by six Ge(Li) detectors positioned at a distance of 20 cm from the target. They were placed symmetrically around the beam direction (fig. 1a) such that for the right and left particle detectors, respectively, four out of the six detectors were at angles of large logarithmic slope of the corresponding γ-ray angular correlations (cf. also fig. 3). The direction of the external polarizing field B_{ext}, oriented perpendicular to the plane spanned by the particle and gamma detectors, was periodically reversed and the measured γ-energies together with the parameters obtained from the particle detectors were accumulated in list mode for the two field directions "up" and "down". The influence of the external field on the

direction of the beam and the scattered particles could be determined experimentally by monitoring the "up - down" count rate differences for the scattered Pb ions in the position sensitive particle detectors. The directional change was determined to be 0.3 ± 0.4 mrad., in agreement with theoretical estimates using average charge states and the measured stray field profile. Similar estimates for recoiling Dy nuclei resulted in correspondingly small directional changes. These changes were consequently neglected in the angular precession analysis.

In the off-line analysis γ-spectra were constructed for each Ge(Li) detector in coincidence with both recoiling Dy and scattered Pb ions. For the Dy-events each particle detector was divided into four angular windows subtending 5^0 in the laboratory frame. The four particle windows correspond to different scattering angles of the recoiling Dy ions and hence to slightly different excitation probabilities of states in the Coulomb excitation process.

The γ-ray energies recorded for Dy-events were corrected for the Doppler shift assuming that the γ-decay takes place outside the backing foil and using the experimentally determined dependence of the energy shifts of the γ-lines on the particle scattering angle. Such a corrected spectrum is shown in fig. 2b for a γ-detector positioned at an average angle of 100^0 with respect to the recoiling Dy nuclei, i.e. close to an angle of maximum

logarithmic slope of the particle-γ angular correlation function. The resulting energy resolution of $\simeq$ 5keV around $E_\gamma = 500$ keV is sufficient to clearly resolve the lines in the backbending region. Full energy peak intensities of the γ-lines were evaluated using standard peak fitting routines which treated the "up" and "down" spectra in an identical manner.

The positions of the particle- and γ-detectors have been chosen symmetrically about the beam axis in order to minimize systematic errors. The symmetry implies that the detection of a γ-ray in detector i in coincidence with a particle at angle θ_p in P_L and polarizing field "up" ("down") corresponds to detecting a γ-ray in detector $j = 7 - i$ in coincidence with a particle at θ_p in P_R and field "down" ("up"). For each observed transition we can hence define double ratios by

$$R_{ij}(\bar{\theta}_p) = \left[\frac{N^{\uparrow}_{iL}(\bar{\theta}_p)}{N^{\downarrow}_{iL}(\bar{\theta}_p)} \cdot \frac{N^{\downarrow}_{jR}(\bar{\theta}_p)}{N^{\uparrow}_{jR}(\bar{\theta}_p)} \right]^{1/2} \qquad (1) \,,$$

where e.g. $N^{\uparrow}_{iL}(\bar{\theta}_p)$ denotes the number of full-energy peak events recorded in γ-detector i in coincidence with particles in detector P_L and polarizing field up, $\bar{\theta}_p$ being the average detection angle for a given par-

ticle window. Obviously the double ratios defined in eq. (1) are sensitive to the precession of the angular correlation but independent of the different γ-detector efficiencies as well as "up" - "down" count rate differences.

For a discussion of the angular correlations $W(\vartheta_\gamma)$ the symmetry is taken into account by adding the (normalized) counting rates for events obtained with the right particle detector to the equivalent rates involving the left particle detector,

$$W^{\uparrow}(\vartheta_\gamma) = \frac{n^{\uparrow}_{iL}(\bar{\theta}_p) + n^{\downarrow}_{jR}(\bar{\theta}_p)}{1/6 \cdot \sum_{i=1}^{6} [n^{\uparrow}_{iL}(\bar{\theta}_p) + n^{\downarrow}_{jR}(\bar{\theta}_p)]} \qquad (2a)$$

and

$$W^{\downarrow}(\vartheta_\gamma) = \frac{n^{\downarrow}_{iL}(\bar{\theta}_p) + n^{\uparrow}_{jR}(\bar{\theta}_p)}{1/6 \cdot \sum_{i=1}^{6} [n^{\downarrow}_{iL}(\bar{\theta}_p) + n^{\uparrow}_{jR}(\bar{\theta}_p)]} \qquad (2b)$$

with j= 7-i. Here e.g. $n^{\uparrow}_{iL}(\bar{\theta}_p)$ is the number of full-energy events $N^{\uparrow}_{iL}(\bar{\theta}_p)$ corrected for the full-energy peak efficiency of the γ-detector i and the up-down as well as left-right count rate differences. The angle ϑ_γ measures the average direction k_γ of the detected γ-ray relative to the average direction k_{Dy} of the recoiling Dy nuclei in the laboratory system (calculated from $\bar{\theta}_p$) for particles detected in the left detector with the convention

$$\operatorname{sgn} \vartheta_\gamma = \operatorname{sgn} \{ (k_{Dy} \times k_\gamma) \cdot B^{\uparrow}_{ext} \} \qquad (3)$$

3. Perturbed Angular Correlations following Multiple Coulomb Excitation

The action of the transient magnetic field B_{tf} on nuclei moving in a ferromagnetic foil can be described as being caused by a classical field which is axially symmetric around the direction of the externally applied magnetic field B_{ext}. The same applies for the static hyperfine field B_{st} acting on ions that have come to rest in the iron foil. Both interactions lead to a precession of angular correlation patterns in a plane perpendicular to B_{ext}. Because of this axial symmetry we shall subseqently calculate the precession effects in a coordinate system with its z-axis oriented in the direction of the external magnetic field B_{ext}. For

Pb-events, where the Dy nuclei are stopped in the iron foil, B_{tf} and B_{st} are assumed, as usual, to be the only extranuclear fields acting on the nucleus. However, for the Dy events, where the excited nuclei recoil into vacuum, an attenuation of the angular correlations might occur which is caused by the hyperfine interaction between the nucleus and the highly ionized and excited atomic shells. This interaction is commonly assumed to be isotropic, i.e. symmetric about any direction.

In order to calculate the particle-γ angular correlations we have to take into account that only the direction (but not the energy) of projectiles or recoiling particles are measured. Thus the feeding from higher lying levels to the state for which the γ-decay is observed has to be considered. All nuclear levels are subsequently assumed to be ordered according to their energies, such that $E_\nu > E_{\nu+1}$. For any state a, populated via Coulomb excitation at t = 0, the initial state m of an observed transition $m \rightarrow n$ can be fed through distinct feeding paths denoted by

$$p^{\mu}_{am} \equiv \{ a,b,\ldots,i,j,k,\ldots,m\}$$

In a coordinate system oriented with $z \parallel B$ the doubly differential cross section for scattering a projectile into Ω and the emission of a γ-ray into Ω_γ within observation times T_1 and T_2 is

$$\frac{d^2\sigma_{mn}(\Omega,\Omega_\gamma,T_1,T_2)}{d\Omega\, d\Omega_\gamma} = \frac{1}{\sqrt{4\pi}} \cdot \left(\frac{d\sigma(\Omega)}{d\Omega}\right)_R \cdot \sum_{\substack{a \le m \\ \mu}} \sum_{k\kappa} \alpha^a_{k\kappa}(\Omega) \cdot H_k(p^{\mu}_{am}) \cdot F_k(I_n I_m) \cdot G_{k\kappa}(p^{\mu}_{am};T_1,T_2) \cdot Y_{k\kappa}(\Omega_\gamma) \qquad (4)$$

where $(d\sigma/d\Omega)_R$ is the Rutherford cross section and $\alpha^a_{k\kappa}(\Omega)$ denote the statistical tensor components for state a at time t = 0 as defined in ref. 11. Note that Ω is the direction of the projectile in a reference frame with $z \parallel B$ having its origin in the centre of mass of the projectile and the target, (c.m.-coordinate system), while Ω_γ is the direction of emission of the γ-ray in a frame having the same orientation but which moves with the excited nucleus (rest-coordinate system). The quantities $H_k(p^{\mu}_{am})$ describe the feeding of state m through the cascade p^{μ}_{am} and are given by:

$$H_k(p^{\mu}_{am}) = \prod_{\substack{i \in p^{\mu}_{am} \\ i \neq m}} U_k(I_j,I_i) \qquad \text{for } a < m \qquad (5)$$

$$= 1 \qquad \text{for } a = m$$

The $U_k(I_j I_i)$ coefficients used here are identical to the $G_k(I_j I_i)$ coefficients defined in ref. 11; moreover, the angular correlation coefficients $F_k(I_n I_m)$ and the spherical harmonics $Y_{k\kappa}(\Omega_\gamma)$ are also defined in accordance with this article.

With the limiting assumptions on the nature of the perturbative interactions outlined above the perturbation coefficients $G_{k\kappa}(p^\mu_{am};T_1,T_2)$ are given by

$$G_{k\kappa}(p^\mu_{am};T_1,T_2) = \int_{T_1}^{T_2} dt_m \cdots \int_0^{t_k} dt_j \cdots \int_0^{t_b} dt_a \qquad (6)$$

$$\cdot \Big[\prod_j \lambda_j e^{-\lambda_j (t_j - t_i)} \Big] \cdot q_k(p^\mu_{am};t_a, \ldots,t_m)$$

$$\cdot \exp\left[-i\kappa \Phi(p^\mu_{am};t_a, \ldots,t_m) \right]$$

with $\lambda_j = \tau_j^{-1}$ defined as the inverse of the total lifetime and t_j as the time when decay $j \to k$ in the cascade p^μ_{am} takes place ($t_j = 0$ for $j = a$). The loss of orientation due to isotropic hyperfine interactions is described by the attenuation factors q_k and the precession effect of the transient and static magnetic fields accumulated in the ferromagnetic foil by the exponential $\exp(-i\kappa\Phi)$. Note that this factorization into an

attenuation factor q_k and a precession factor $\exp(-i\kappa\Phi)$ is possible because the fields responsible for the attenuation and the interaction causing the precession act at different times. For the present experiment the limits T_1 and T_2 of the time integration have to be chosen in the following way: As the Doppler correction procedure for Dy-events described in sect. 2 assumes the recoil velocities as measured on exiting from the ferromagnetic foil (neglecting the very small transit time through the Al-layer), only γ-rays from transition $m \to n$ occuring at times $t_m \geq t_{tr}$ are properly corrected and contribute to the γ-line, hence $T_1 = t_{tr}$ and $T_2 = \infty$. In the Pb-events, where the corresponding Dy nuclei come to rest in the iron within the stopping time t_s, any γ-rays emitted during the slowing down process in the iron foil are not to be considered since only the stopped peak (but not the full Doppler-broadened line shape) was integrated and therefore $T_1 = t_s$ and $T_2 = \infty$ in this case.

The total precession angle $\Phi(p^\mu_{am};t_a,\ldots,t_m)$ is the sum of the differential precessions $\Phi_j(t_j,t_i)$ the nucleus experiences due to the interaction of the magnetic moment of the state j with the magnetic field during the time interval between its population at time t_i and decay at time t_j:

$$\Phi(p^\mu_{am};t_a,\ldots,t_m) = \sum_{j \in p^\mu_{am}} \Phi_j(t_j,t_i) \qquad (7a)$$

with

$$\Phi_j(t_j,t_i) = -(\mu_N/\hbar)\, g_j \int_{t_i}^{t_j} B(t')dt' \qquad (7b)$$

where μ_N denotes the nuclear magneton and g_j the g-factor of the state j in the cascade p^{μ}_{am} ; B(t') is the magnetic field acting on the nucleus at time t', i.e. B(t') = 0 if the nucleus is outside the iron at time t', $B(t') = B_{st}$ for nuclei at rest in the iron, and $B(t') = B_{tf}(v(t'))$ for nuclei recoiling in the iron foil with velocity v at time t'.

For the functional dependence of the transient field $B_{tf}(v)$ for Dy nuclei (Z = 66) recoiling in iron we have used the parametrization given in ref. 12:

$$B_{tf}(v) = a \cdot Z\,(v/v_o) \cdot \exp -[\beta(v/v_o)] \qquad (8)$$

with a = +19.0 T and β = 0.12. This calibration has been determined from transient field experiments involving nuclei in this mass region and recoil velocities $v/v_o \leq 10.5$ assuming no Coulomb scattering (Lindhard - Winther) contribution to be present; the error of $B_{tf}(v)$ in this velocity region is quoted in ref. 12 to be of the order of ± 5% . The inclusion of a Lindhard - Winther field changes the parameters to a= +15.5 T and β = 0.10, respectively: the effect of including a Lindhard - Winther term in the analysis of the Pb-event data shall be discussed in sect. 4.2.

For a proper application of the field strength parametrization, the stopping powers dE/dx needed to derive the function v(t') must be the same as those used in the calibration, and consequently we have used the dE/dx values of ref. 12.

The spin relaxation processes resulting from hyperfine interactions are assumed to occur for nuclei recoiling in vacuum only, therefore for Pb-events the attenuation coefficients $q_k(p^{\mu}_{am};t_a,\ldots,t_m)$ are set equal to unity. For the Dy-events, however, a simple exponential time dependence was assumed for $t > t_{tr}$, i.e.:

$$q_k(p^{\mu}_{am};t_a,\ldots,t_m) = 1 \qquad \text{for } t_m \leq t_{tr} \qquad (9a)$$

and

$$q_k(p^{\mu}_{am};t_a,\ldots,t_m) = \exp\,[-k(k+1) \cdot \Lambda_m \cdot (t_m - t_{tr})] \qquad \text{for } t_m > t_{tr} \qquad (9b)$$

This corresponds to an Abragam and Pound type behaviour[13] for purely magnetic interactions, assuming an average g-factor for all the levels in the various possible feeding paths leading to state m; effective attenuation parameters Λ_m could be determined from the present experiment (see sect. 4.1).

A computer code was developed which performs the evaluation of the multiple integrals occuring in eq. (4) by a Monte Carlo integration method. This method allows in a simple way to include all experimental constraints determined by the experimental set-up and the mode of data analysis. The statistical tensors $\alpha^{a}_{kK}(\Omega)$, which determine the population of the states at time t = 0, are calculated by means of a slightly modified Winther-de Boer code [11] taking the relevant electromagnetic matrix elements and other spectroscopic informations for ^{158}Dy and ^{164}Dy, respectively, from our previous experiments [3,8,14]. In ^{158}Dy, in particular, all side bands are found to be only very weakly Coulomb excited as compared to the yrast band; consequently the feeding of the yrast states from sidebands can be neglected in the analysis. In order to calculate the γ-ray yields observed in a particular coincidence configuration Ω_γ and Ω have to be transformed into the laboratory frame and finally an integration over the solid angles of the particle and gamma detector has to be performed. Note, however, that the integration over the solid angle of the γ-detectors leads to negligible attenuations of the angular correlations as the γ-detectors are positioned at far distances from the target.

The procedure described above allows the calculation of the particle-γ angular correlations and the up/down double ratios both for nuclei which recoil into vacuum as well as for those which come to rest in the iron

foil. The final results presented in section 4 were derived using this procedure. For clarity purposes, however, approximate results in terms of average precession angles will also be presented.

4. *Analysis and Results*

4.1 Attenuation in vacuum

As the first step in the data analysis the attenuation of the γ-angular correlations due to hyperfine interactions for ions recoiling in vacuum was investigated by comparing the experimentally determined angular correlations for Dy-events to those calculated for various assumptions on the effective attenuation parameter Λ_m.
For this purpose the experimental angular correlation functions $W(\vartheta_\gamma)$ were deduced for the yrast transitions in ^{158}Dy using eq. (2) and averaging over $W^{\uparrow}(\vartheta_\gamma)$ and $W^{\downarrow}(\vartheta_\gamma)$ as well as over two adjacent particle windows.

The theoretical cross-sections were calculated as described in sect. 3 and compared to $W(\vartheta_\gamma)$ after performing the same averaging and normalization procedure. For this comparison the g-factors entering via eq. (7) were assumed to be constant, $g_j = 0.35$, but the averaged $W(\vartheta_\gamma)$ turn out to be

independent of the choice of g_j mainly because the accumulated precessions are small and moreover cancel in first order by the up/down averaging procedure. For high spin state transitions with $I_m^\pi \geq 12^+$ the experimental angular correlation functions are found to be well represented by the corresponding theoretical correlations assuming $\Lambda_m=0$, i.e. no attenuation is observed for these transitions (cf. fig. 3b). For the decays between the low spin states with $I_m^\pi \leq 10^+$, however, the attenuation is increasing with decreasing spin (cf. fig. 3a), the $4^+ \rightarrow 2^+$ transition being consistent with an isotropic angular correlation pattern in the rest-coordinate system. Within the accuracy of the angular correlation data, which is predominantly determined by the knowledge of the relative efficiencies between the six Ge-detectors, no velocity dependence of Λ_m for the two sets of data with $20° \leq \theta_{Dy} \leq 30°$ and $30° \leq \theta_{Dy} \leq 40°$, corresponding to average recoil velocities of 10.7 v_o and 8.4 v_o, respectively, was observed. Averaged values of Λ_m are given in table 1.

As can be seen from table 1 the effective attenuation parameters deduced for low spin state transitions with $I_m^\pi \leq 10^+$ are independent of m, the average value being $\overline{\Lambda} = 0.024 \pm 0.004$ ps^{-1}. This value is in agreement with what has been observed for low spin state transitions in other heavy nuclei recoiling into vacuum at similar velocities[15]. The increasing insensitivity of high spin state transitions to the hyperfine interaction

is due to the short lifetimes of the high spin yrast states. In fact the corresponding angular correlations are found to be consistent with $\Lambda_m \simeq \overline{\Lambda}$ as well as $\Lambda_m \simeq 0$, which are the values expected if the average g-factor of the high spin states is of the order of that of the low spin states or approximately zero, respectively. Using the average attenuation parameter $\overline{\Lambda}$ not only the normalized angular correlations but also the relative intensities of the yrast transitions are well reproduced by our calculations, which also confirms the set of matrix elements used in the Coulomb excitation calculation and the evaluation of the subsequent decay.

4.2 Large impact parameter data: Pb-events

Gamma spectra in coincidence with Pb-events correspond to large impact parameters with the Dy ions excited to low spin levels only ($I^\pi \leq 10^+$, see fig. 2a). They recoil at large angles with respect to the beam direction, are stopped inside the ferromagnetic foil and therefore also experience the static hyperfine field B_{st}(Dy<u>Fe</u>) in addition to the transient field B_{tf}.

The transient field strength was derived from the parametrization given by eq. (8), but as various calibrations (see e.g. ref. 9) yield quite similar

precession estimates for recoil velocities relevant in this case ($v \leq 7v_o$), the results for the g-factors obtained from the Pb-events do not depend on the choice of this parametrization. In view of the uncertainties connected with the possible presence of a Lindhard - Winther contribution to the transient field the consequences of including a Lindhard - Winther term in the transient field calibration were also investigated.

The angular precessions observed for the stopped Dy ions were analyzed for yrast transitions in ^{158}Dy and for ^{164}Dy, using the ^{164}Dy data mainly to determine $B_{st}(Dy\underline{Fe})$. The g-factor of the 2_1^+ level of ^{164}Dy is known[16] to be $g(2^+) = 0.35 \pm 0.02$; assuming - as seems justified for ^{164}Dy being a good rotor - the same value for the g-factor of the 4_1^+-state with $\tau(4^+) = 286 \pm 15$ ps (ref. 17) (the $2^+ \rightarrow 0^+$ transition has not been observed) - the value of the static field of Dy in Fe is determined from the precession of the $4^+ \rightarrow 2^+$ transition to be $B_{st}(Dy\underline{Fe}) = -245 \pm 25$ T (see fig. 4a). As this value slightly exceeds an earlier result of $B_{st}(Dy\underline{Fe}) = -160 \pm 30$ T, - re-evaluated from ref. 18 using the g-factor and lifetime quoted here - , it does prove that under the kinematical conditions required for the Pb-events all recoiling Dy nuclei came to rest in the iron foil and that the ^{208}Pb beam did not deteriorate the magnetization of the iron foil throughout the experiment.

Using the value of $B_{st}(Dy\underline{Fe}) = -245 \pm 25$ T, the g-factors of some low spin states in ^{158,164}Dy could be determined from the angular precession data. For the 6^+ state in ^{164}Dy with $\tau(6^+) = 39 \pm 1.9$ ps (ref. 17) a value of $g(6^+) = +0.28 \pm 0.08$ was obtained. The value deduced for the g-factor of the 4^+ level in ^{158}Dy is $g(4^+) = +0.35 \pm 0.06$ (see fig. 4b) in agreement with the result of an earlier recoil-in-Gd measurement[19]. It is worth noting that the transient field contribution to the precession of these long lived states is much smaller than that from the static field, hence possible uncertainties regarding the transient field at low velocities[9] do not influence the above results. For the 6^+ level in ^{158}Dy having a lifetime of 13.1 ps, the contribution from the static field should be compensated by the transient effect being of opposite sign. Using the parametrization of eq. (8) the net precession is expected to be very close to zero, in excellent agreement with what is observed experimentally. Because of this cancellation, the g-factor of the 6^+ state in ^{158}Dy cannot be determined from the data, however, as $g(6^+)$ is expected to be $\neq 0$ (see also sect. 4.3), it proves that the transient field effect is present and that the average size of the field is consistent with what is obtained from eq. (8); for $g(6^+) \approx g_c = 0.35$ the consistency can be estimated to be better than ± 20 % within the relevant velocity region $0 \leq v/v_o \leq 7.0$.
Finally for the 8^+ state in ^{158}Dy, where the transient precession effect exceeds the static field precession because of the shorter lifetime of

$\tau(8^+) = 4.2$ ps, the analysis yields a g-factor of $g(8^+) = + 0.41 \pm 0.13$. This is the only state where including a Lindhard - Winther term in the transient field calibration could affect the deduced g-factor. With the parametrization quoted above we derive $g(8^+) = + 0.39 \pm 0.13$.

It should be pointed out that in the analysis of the large impact parameter data effects due to feeding via preceding yrast states could be neglected. This is beause both the direct population as well as the lifetimes of the states involved are rapidly decreasing with increasing spin.

4.3 Low impact parameter data: Dy-events

For the Dy-events the double ratios defined in sect. 2 were constructed for each of the four particle windows. As can be seen from fig. 3, four double ratios are maximally sensitive to the precessions of the angular correlation patterns. For reasons of statistics the Dy-events could only be analyzed for the measurement performed on ^{158}Dy.

The velocity range of the Dy ions in the Fe foil ($7 \leq v/v_o \leq 14$) is determined by taking the entrance velocity from the kinematics of the Coulomb excitation process and the exit velocity directly from the observed γ energy shifts; both velocities vary with the recoil angle of the Dy ions.

Although the parametrization of the transient field given by eq. (8) is based only on experiments involving ion velocities of $v/v_o \leq 10.5$, which overlaps just with the lower half of the velocity range spanned by the Dy ions, we retained eq. (8) as parametrization for the transient field acting at the highest velocities occuring in the present experiment; it is felt that the assumed error of 20% in the transient field strength at these velocities should account for possible uncertainities connected with this extrapolation. Moreover, an independent check of the strength of the transient field at high velocities was obtained from a recent ^{25}Mg(^{136}Xe,5n)^{156}Dy transient field experiment[20] at E_{Xe}=4.7 MeV/u. The measurement was performed using a recoil-distance set-up with a thin, backed iron foil as a "stopper". By varying the distance between the Mg target and the Fe foil the population of the states experiencing the transient field could be controlled. Angular precession values observed for the 6^+ and 4^+ yrast transition and a level population centered around the $I^\pi=6^+$ yrast level in ^{156}Dy determine the strength of the transient field in the velocity range $4 \leq v/v_o \leq 11$ to be within 20% of the value obtained with the above parametrization (assuming a collective g-factor of $g_c \approx 0.35$ for the states involved).

In order to demonstrate the main implications of the present data, we first present approximate results in terms of average precession angles. Table 2 shows the precession angles, averaged over the four particle win-

dows and the four γ-detector pair combinations, for the various γ-transitions. They were derived as e. g. described in ref. 9 from the double ratios and calculated slopes of the angular correlations in the rest frame of the decaying nucleus, using effective attenuation parameters of $\Lambda_m = \overline{\Lambda}$ = 0.024 ps^{-1} for all transitions (see sect. 4.1). Since the transit times of the Dy ions in the Fe foil are short compared to the lifetimes of the nuclear states involved, in good approximation all decays occur after the emergence of the ions from the ferromagnetic foil. The precession measured for a particular transition m → n therefore includes the precessions in all preceding states a ≤ m weighted by their direct population probabilities. With the transient field as given in eq. (8) the assumption of a constant collective g-factor of +0.35 leads to an average precession of $-\bar{\Phi}$ = 20 mrad. The observed precession angles (table 2) indicate a significant reduction of the g-factors consistent with g ≈ 0 for the 10^+-16^+ levels, the conclusion being independent of the particular choice of the effective attenuation factors as well as possible uncertainities in the size of the transient field at high recoil velocities.

The quantitative analysis was carried out in the manner described in section 3; the Monte-Carlo calculations were performed for various values of the g-factors of the high-spin levels and compared to the experimental double ratios for the four particle angular windows and the sensitive

γ-detector pairs. The statistical accuracy of this experiment only allowed the extraction of an average g-factor for the high spin states. This average g-factor is representative for the high spin states at backbending, since the experiment is mostly sensitive to the 14^+ and 16^+ levels. The lower part of fig. 5 represents the sensitivity (as determined from the γ-ray yields) of the present experiment to the g-factors of the various levels. The average spin is determined to be <I>=14.1 with 75% of the sensitivity concentrated at spins 12^+, 14^+ and 16^+. The g-factor of the 8^+ level was fixed at the collective value of $g(8^+)$=0.35, in agreement with the experimental result (cf. sect. 4.2). The average g-factor for the 10^+-16^+ levels was thus determined to be g= +0.04 ± 0.11, where the error includes the uncertainty in the transient field strength. The calculations were carried out assuming the effective attenuation parameters $\Lambda_m = \overline{\Lambda}$ = 0.024 ps^{-1} for all states; note, however, that the result does not depend on this choice of Λ_m for the high spin state transitions for reasons given above (cf. sect. 4.1). Although the g-factor of the 10^+ level is most probably different from $g(10^+) \approx 0$, changes in the value of $g(10^+)$ (and likewise of $g(8^+)$) do not affect the result for the average g-factor in any significant way as the 10^+ state contributes only 10% to the overall sensitivity; the assumption of a larger value of $g(10^+)$ would result in a slightly larger reduction of the average g-factor of the higher levels compared to the collective value.

5. *Discussion*

The g-factors resulting from the present experiment are summarized in table 3 and displayed in fig. 5.

The main conclusion of the present experiment is that the g-factors of the high spin yrast levels in the backbending region of ^{158}Dy are significantly reduced (consistent with g = 0) as compared to the average value of g≃ +0.35 observed for the low spin members of the yrast sequence in ^{158}Dy as well as ^{164}Dy. We have measured the in-beam magnetization of the Fe foil (via the static hyperfine field of Dy in Fe) and have shown that the transient field was acting throughout the measurement (sect. 4.2). We have furthermore shown that the angular correlations of the high spin transitions are highly anisotropic and not noticably attenuated by the hyperfine interaction in vacuum. The transient field has been taken from an existing parametrization determined from measurements using similar ions[12]; an extrapolation was needed only for the highest velocity range ($10.5v_o \leq v \leq 14v_o$) while the lower velocities span the range where the adopted parametrization has been experimentally verified. Moreover, a recent experiment with ^{156}Dy ions[20] experiencing the transient field at the same high velocities $4v_o \leq v \leq 11v_o$ agrees with the adopted parametrization to

within ~20%. Thus the small precessions observed for the high spin states have to be attributed to g-factors close to zero.

The observed reduction of the g-factors in the backbending region of ^{158}Dy constitutes a stringent test of the rotation alignment picture, in which the main cause of the lowest discontinuities observed in the yrast sequence of many deformed rare earth nuclei are attributed to the successive alignment of pairs of quasiparticles in high-j intruder orbits: The measured average g-factor of g= +0.04 ± 0.11 directly demonstrates that the alignment of an $i_{13/2}$ *neutron* pair rather than of an $h_{11/2}$ *proton* pair plays the dominant role in the intrinsic structure of the yrast states in the first backbending region of ^{158}Dy. Furthermore, the amount of the observed reduction requires that the aligned neutron pair has a large spin component i along the axis of collective rotation: using the simplified expression of ref. 4 - relating the g-factors of yrast states to the aligned angular momenta of quasiparticles - an aligned angular spin of i ≃ 10 ħ is obtained, which is close to the maximum possible aligned spin of i = 12 ħ obtainable by complete alignment of an $i_{13/2}$ neutron pair. The extracted value of i ≃ 10 ħ is slightly larger than the one deduced from the energies of the yrast levels in ^{158}Dy (ref. 2), although both values are presumably still consistent in view of the uncertainities and approximations made in both procedures used to extract i (see also the recent, more detailed discussion of Chen and Frauendorf[21] on the connection

between level energies, g-factors and aligned angular momenta in terms of the Cranked Shell Model approach).

Theoretical g-factor predictions for ^{158}Dy and ^{164}Dy obtained from Cranked-HFB calculations by Diebel et al.[22] are in fair agreement with the experimental results (see fig. 5), although the slightly larger observed reduction of the average g-factor around spin 14^+ might indicate again that the amount of aligned angular momentum produced by the $i_{13/2}$ neutron quasiparticle pair is somewhat larger than $\simeq 7.5\ \hbar$, which is the corresponding weighted average obtained in the CHFB calculations of Diebel et al..

This work was supported in part by the Bundesministerium für Forschung und Technologie.

References

1. P. Thieberger, A.W. Sunyar, P.C. Rogers, N. Lark, O.C. Kistner, E. der Mateosian, S. Cochavi and E.H. Auerbach, Phys.Rev.Lett. *28* (1972) 972

2. R. Bengtsson and S. Frauendorf, Nucl.Phys. *A314* (1979) 27; Nucl.Phys. *A327* (1979) 139

3. H. Emling, E. Grosse, D. Schwalm, R.S. Simon, H.J. Wollersheim, D. Husar and D. Pelte, Phys.Lett. *98B* (1981) 169

4. S. Frauendorf, Phys.Lett. *100B* (1981) 219

5. K.-H. Speidel, G.J. Kumbartzki, W. Knauer, R. Kuhnen, G. Kraft, J. Gerber, M.B. Goldberg, G. Goldring and A. Zemel, Nucl.Phys. *A344* (1980) 176

6. H.R. Andrews, O. Häusser, D. Ward, P. Taras, N. Rud, B. Haas, R.M. Diamond, P. Fossan, H. Kluge, M. Neiman, C. Roulet and F.S. Stephens, Phys.Rev.Lett. *45* (1980) 1835

7. A. Zemel, C. Broude, E. Dafni, A. Gelberg, M.B. Goldberg, J. Gerber, G.J. Kumbartzki and K.-H. Speidel, Nucl.Phys. *A383* (1982) 165

8. H. Emling, P. Fuchs, E. Grosse, R. Kulessa, D. Schwalm, R.S. Simon and H.J. Wollersheim, Int. Conf. on Nuclear Behaviour at High Angular Momentum, Strasbourg, 1980

9. N. Benczer-Koller, M. Hass and J. Sak, Ann.Rev. of Nucl. and Part.Sci. *30* (1980) 53 and references therein

10. P. Fuchs, Ph.D. Thesis, to be published; see also D. Schwalm, Proc. Int. Summer School on Nuclear Structure, Dronten, 1980 in Nuclear Structure, ed. K. Abrahams, K. Allaart, and A.E.C. Dieperink (Plenum Press, New York and London 1981) p. 207

11. A. Winther and J. de Boer, in Coulomb Excitation, ed. K. Alder and A. Winther (Acad. Press, New York, 1966) p. 303

12. H.R. Andrews, O. Häusser, D. Ward, P. Taras, R. Nicole, J. Keinonen, P. Skensved and B. Haas, Nucl.Phys. *A383* (1982) 509; O. Häusser, private communication

13. G. Goldring, Hyp. Int. *5* (1978) 283 and references therein

14. H.J. Wollersheim, H. Emling, P. Fuchs, E. Grosse and D. Schwalm, Int. Conf. on Band Structure and Nuclear Dynamics, New Orleans, 1980 and to be published

15. Ch. Michel, H. Emling, E. Grosse, R. Piercey, D. Schwalm, G. Seiler-Clark, J. Stachel and H.J. Wollersheim, GSI Scientific Report 1981, Darmstadt

16. Table of Isotopes, ed. C.M. Lederer and V.S. Shirley (John Wiley & Sons, New York, 1978); the adopted value is the average of the results quoted in this reference.

17. R.O. Sayer, E. Eichler, N.C. Singhal, R. Sturm, N.R. Johnson and M.W. Guidry, Phys.Rev. *C17* (1978) 1026

18. L. Grodzins, R. Borchers and G.B. Hagemann, Phys.Lett. *21* (1966) 214

19. R. Kalish, B. Herskind and G.B. Hagemann, Phys.Rev. *C8* (1973) 757

20. H. Emling, H. Grein, E. Grosse, R. Kulessa, C. Michel, D. Schwalm,

G. Seiler-Clark, M. Hass, G.J. Kumbartzki and K.-H. Speidel, to be published

21. Y.S. Chen and S. Frauendorf, preprint

22. M. Diebel, A.N. Mantri and U. Mosel, Nucl.Phys. *A345* (1980) 72

Figure Captions

Fig. 1: a) Schematic view of the experimental set-up consisting of six Ge detectors and two (P_L and P_R) position sensitive parallel plate detectors. The dashed line represents a typical γ-angular correlation in the laboratory frame for Dy ions detected in P_L. The polarizing magnetic field B_{ext} is perpendicular to the detector plane shown; the "up" direction corresponds to B_{ext} pointing out of this plane towards the reader.

b) Details of the structure of the targets used together with a sketch of the two types of events ("Dy- and Pb-events", see also text) considered in the analysis. Note that the Pb-events were restricted to scattering angles $20^\circ \leq \theta_{Pb} \leq 27^\circ$ in order to ensure that the corresponding Dy ions are stopped in the iron foil.

c) Scatter-plot of time-of-flight vs. scattering angle; the Fe, Dy and Pb ions are well separated. The Fe-events are partly suppressed by a threshold on the anode pulse of the particle detector.

Fig. 2: a) Gamma-ray spectrum of ^{158}Dy observed in detector 4 in coincidence with Pb ions detected in P_L between $20^\circ \leq \theta_{Pb} \leq 27^\circ$. The

marked γ-ray lines correspond to the decay of ^{158}Dy being at rest in the iron foil, while the lower energy satellites are due to Dy-events, which were not completely suppressed by the time-of-flight window used in the analysis.

b) Gamma-ray spectrum observed in detector 4 in coincidence with ^{158}Dy ions detected in P_R between $30^0 \leq \Theta_{Dy} \leq 40^0$. The marked γ-ray lines correspond to the decay of the yrast states of ^{158}Dy after emergence from the target.

Fig. 3: a) The γ-angular correlation $W(\vartheta_\gamma)$ (in the laboratory frame) for the $8^+ \rightarrow 6^+$ yrast transition in ^{158}Dy, observed in coincidence with Dy ions detected at $20^0 \leq \Theta_{Dy} \leq 30^0$ The solid line represents Coulomb excitation calculations including the attenuation due to hyperfine interactions present while the Dy nuclei recoil in vacuum. The dashed line refers to the unperturbed correlation.

b) Same for the 12^+-10^+ yrast transition in ^{158}Dy. The solid line represents the unperturbed correlation.

In the lower panels the corresponding up-down double ratios (cf. eq. (1)) are displayed, which were calculated by assuming a constant g-factor of g = 0.35 for all levels involved.

The arrows indicate the actual positions of the four Ge-detectors most sensitive to the presession.

Fig. 4: a) Gamma-angular correlation of the $4^+ \rightarrow 2^+$ yrast transition in ^{164}Dy for Dy ions decaying after being stopped in the iron foil (Pb-events) with polarizing field "up" (full circles) and "down" (open circles), respectively. The solid and dashed lines represent the best fit obtained with $g(4^+)=0.35$ and adjusting the static hyperfine field strength B_{st}(Dy<u>Fe</u>). The fit results in B_{st}(Dy<u>Fe</u>) = -245 ± 25 T.

b) Same for the $4^+ \rightarrow 2^+$ yrast transition in ^{158}Dy. The best fit yields $g(4^+)=+0.35 \pm 0.06$ using B_{st}(Dy<u>Fe</u>) as determined above.

Fig. 5: Summary of the g-factor results obtained in the present experiment for yrast states in ^{158}Dy and ^{164}Dy. For the 10^+ to 16^+ levels in ^{158}Dy only an average g-factor has been deduced. The lower part of the figure displays the sensitivity of this average value to the various yrast levels in ^{158}Dy as determined from experimental γ-ray intensities. The dashed line represents a theoretical prediction of the g-factors for the yrast states in ^{158}Dy and the dotted line the predictions for ^{164}Dy (ref.22).

Tables

Table 1

Effective attenuation parameters Λ_m derived from the measured angular correlations for yrast transitions in ^{158}Dy

transition $I_m^\pi \rightarrow I_n^\pi$	E_γ(keV)[a]	τ_m (ps)[a]	Λ_m (ps^{-1})
$4^+ \rightarrow 2^+$	218.2	103 ± 7	-
$6^+ \rightarrow 4^+$	320.6	13.1 ± 1.5	0.023 ± 0.005
$8^+ \rightarrow 6^+$	406.3	4.2 ± 0.8	0.022 ± 0.005
$10^+ \rightarrow 8^+$	476.0	2.03 ± .27	0.027 ± 0.010
$12^+ \rightarrow 10^+$	529.3	1.23 ± .23	< 0.04
$14^+ \rightarrow 12^+$	563.4	1.05 ± .22	< 0.04
$16^+ \rightarrow 14^+$	578.1	0.91 ± .13	< 0.04

a) from ref. 3

Table 2:

Average precession angles $\bar{\Phi}$ derived from ^{158}Dy events

transition $I_m^\pi \rightarrow I_n^\pi$	$-\bar{\Phi}$(mrad)
$8^+ \rightarrow 6^+$	+ 16 ± 5
$10^+ \rightarrow 8^+$	+ 1.4 ± 5.3
$12^+ \rightarrow 10^+$	+ 0.6 ± 5.7
$14^+ \rightarrow 12^+$	+ 6 ± 11
$16^+ \rightarrow 14^+$	- 46 ± 24

Table 3:

Summary of g-factors determined in the present experiment.

state I^{π}	^{158}Dy	^{164}Dy
2^+	--	+0.35 ± 0.02[a]
4^+	+0.35 ± 0.06	--
6^+	--	+0.28 ± 0.08
8^+	+0.41 ± 0.13	--
10^+-16^+	+0.04 ± 0.11[b]	--

[a] ref 10.

[b] The average spin is <I> = 14.1 (see fig.5)

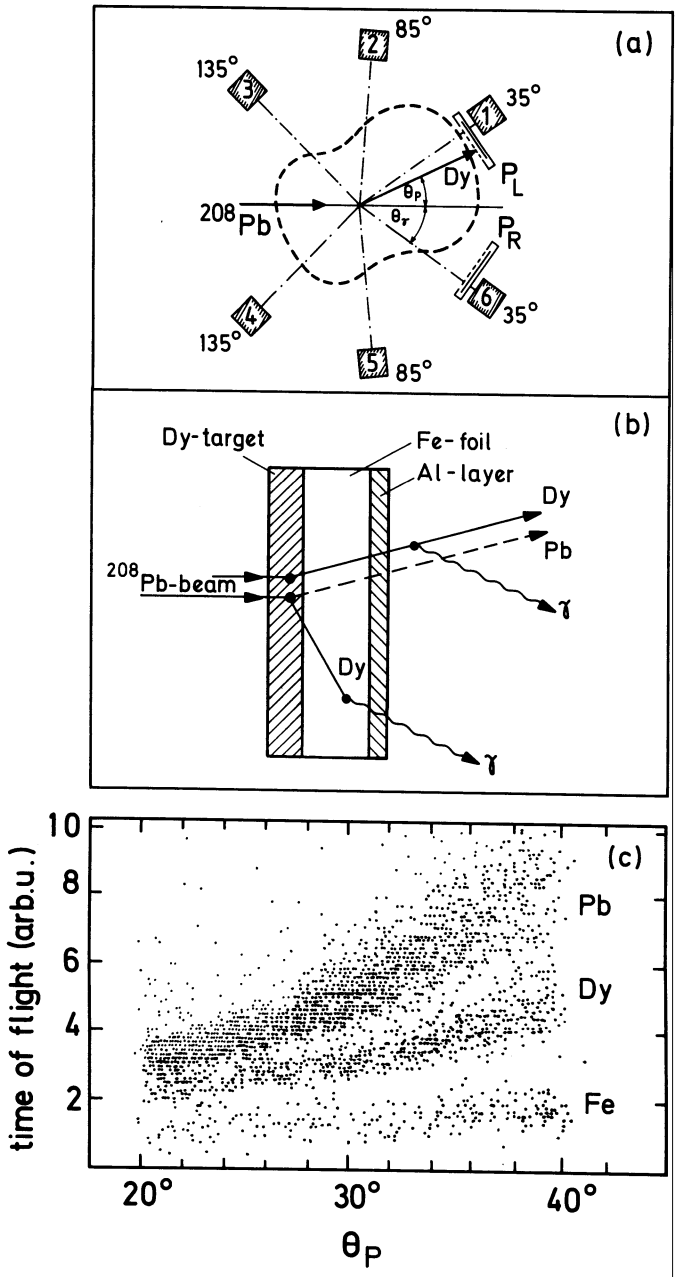

Fig.1

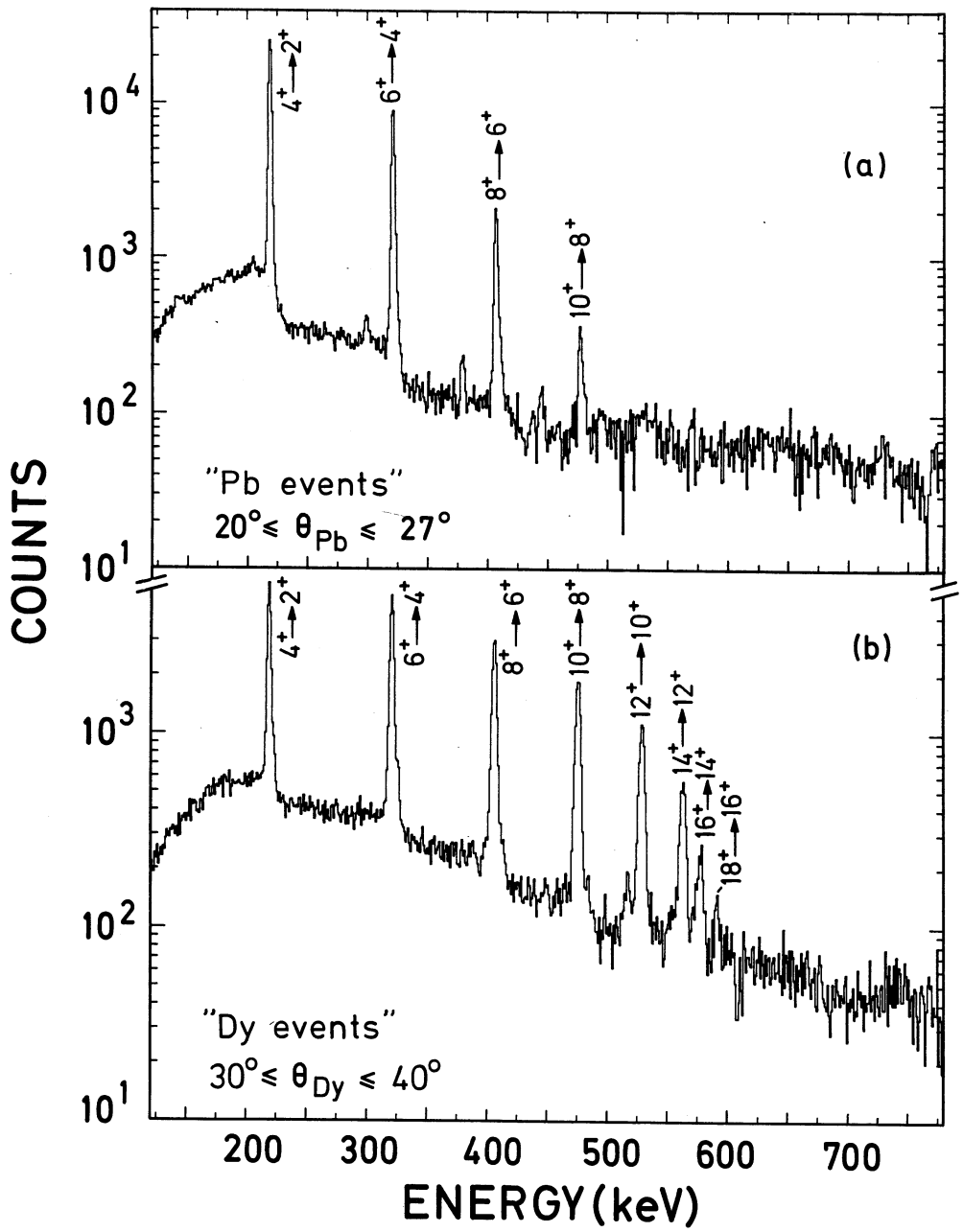
COUNTS
ENERGY (keV)
(a)
(b)
"Pb events"
20° ≤ θPb ≤ 27°
"Dy events"
30° ≤ θDy ≤ 40°
4+→2+
6+→4+
8+→6+
10+→8+
12+→10+
14+→12+
16+→14+
18+→16+

Fig.2

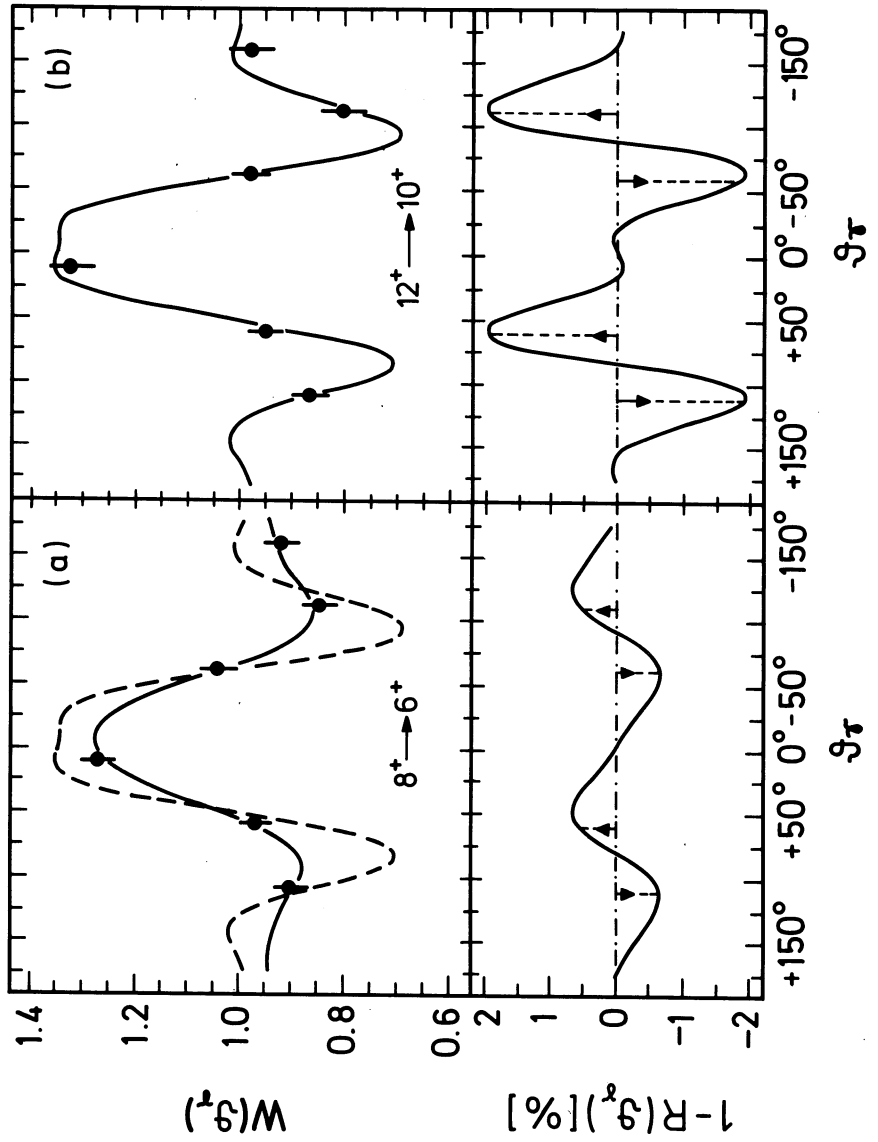
(a)
(b)
8+→6+
12+→10+
W(ϑτ)
1-R(ϑτ)[%]
ϑτ

Fig.3

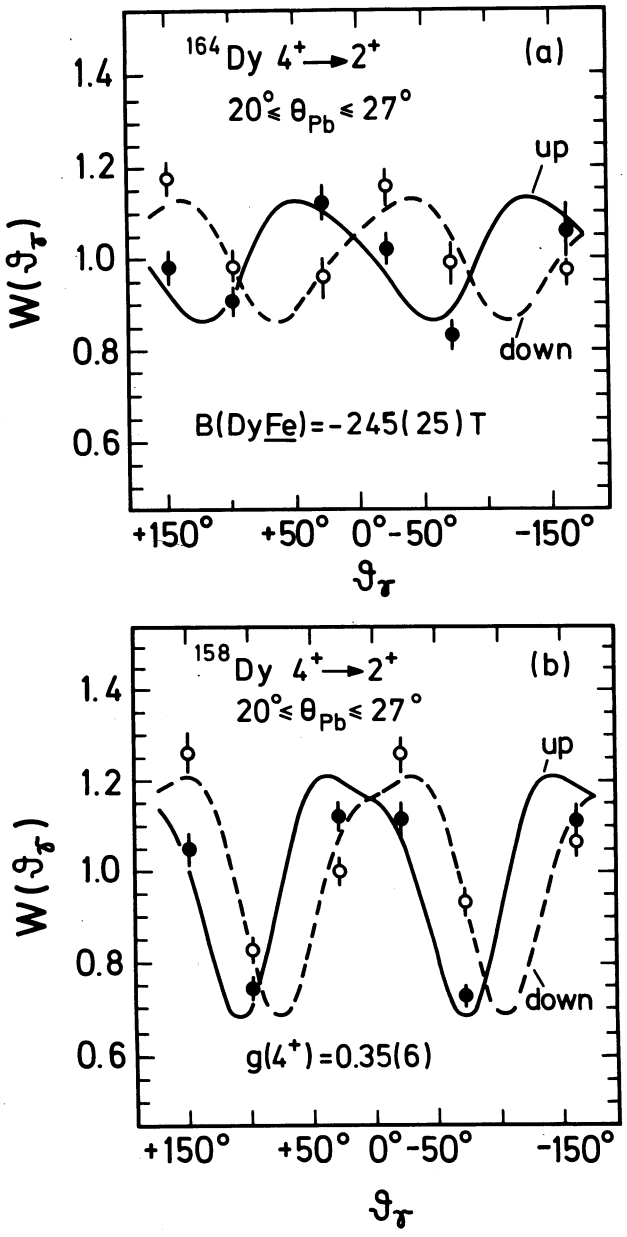
^{164}Dy 4$^+$→2$^+$
(a)
20°≤ θ$_{Pb}$ ≤27°
up
down
B(DyFe)=-245(25) T
W(ϑ$_\gamma$)
ϑ$_\gamma$
+150° +50° 0° -50° -150°
1.4
1.2
1.0
0.8
0.6
^{158}Dy 4$^+$→2$^+$
(b)
20°≤ θ$_{Pb}$ ≤27°
up
down
g(4$^+$)=0.35(6)

Fig.4

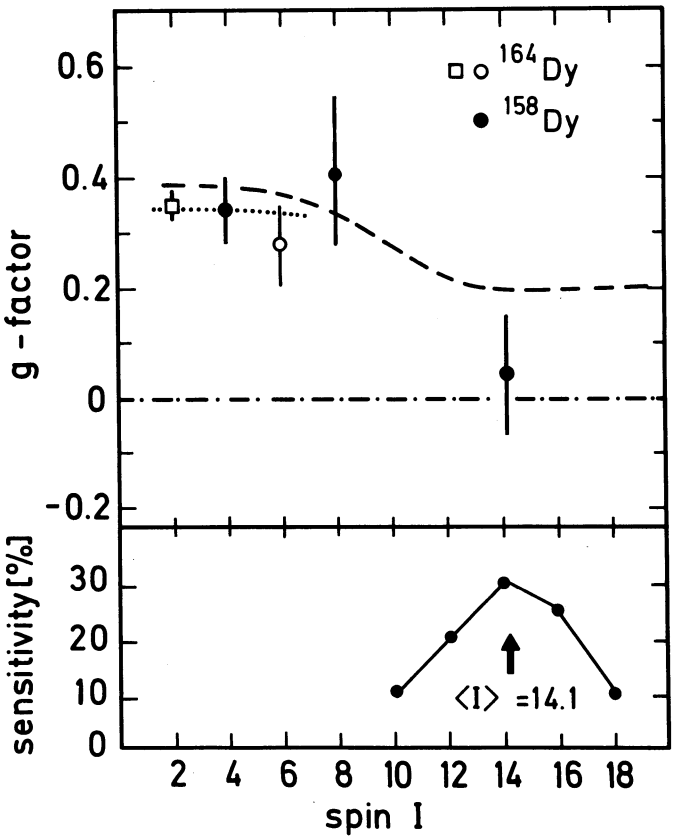
□ ○ ^{164}Dy
● ^{158}Dy
g - factor
0.6
0.4
0.2
0
-0.2
sensitivity [%]
30
20
10
0
<I> =14.1
2 4 6 8 10 12 14 16 18
spin I

Fig.5